REPORT DOCUMENTATION PAGE

Form Approved
OMB No. 0704-0188

Public reporting burden for this collection of information is estimated to average 1 hour per response, including the time for reviewing instructions, searching existing data sources, gathering and maintaining the data needed, and completing and reviewing the collection of information. Send comments regarding this burden estimate or any other aspect of this collection of information, including suggestions for reducing this burden, to Washington Headquarters Services, Directorate for Information Operations and Reports, 1215 Jefferson Davis Highway, Suite 1204, Arlington, VA 22202-4302, and to the Office of Management and Budget, Paperwork Reduction Project (0704-0188), Washington, DC 20503.

1. AGENCY USE ONLY (Leave blank)	2. REPORT DATE	3. REPORT TYPE AND DATES COVERED
		FINAL REPORT 15 Nov 94 - 14 Nov 95

4. TITLE AND SUBTITLE
Structure and Dynamics of Excited Atoms

5. FUNDING NUMBERS
61102F
2301/DS

AFOSR-TR-96
0044

6. AUTHOR(S)
Professor T. F. Gallagher

7. PERFORMING ORGANIZATION NAME(S) AND ADDRESS(ES)
Jesse W. Beams Laboratory of Physics
University of Virginia
Charlottesville, Virginia 22901

8. PERFORMING ORGANIZATION REPORT NUMBER

9. SPONSORING/MONITORING AGENCY NAME(S) AND ADDRESS(ES)
AFOSR/NE
110 Duncan Avenue Suite B115
Bolling AFB DC 20332-0001

10. SPONSORING/MONITORING AGENCY REPORT NUMBER
F49620-95-1-0034

11. SUPPLEMENTARY NOTES

12a. DISTRIBUTION/AVAILABILITY STATEMENT
APPROVED FOR PUBLIC RELEASE: DISTRIBUTION UNLIMITED

12b. DISTRIBUTION CODE

13. ABSTRACT (Maximum 200 words)

Our efforts under AFOSR grant F49620-95-1-0034 have been focused on two topics, resonant collisional energy transfer between cold Rydberg atoms and microwave multiphoton processes in Rydberg atoms. In both of these lines of research we are taking advantage of the exaggerated properties of Rydberg atoms to explore physical regimes which would be hard to study quantitatively in other systems. For example in the collision experiments with cold Rydberg atoms we hope to see the evolution from two body collisions to many body interactions as we increase the strength of the interaction between atoms.

19960206 069

14. SUBJECT TERMS
Cold Rydberg Atoms, Microwave Multiphoton Processes

15. NUMBER OF PAGES

16. PRICE CODE

17. SECURITY CLASSIFICATION OF REPORT	18. SECURITY CLASSIFICATION OF THIS PAGE	19. SECURITY CLASSIFICATION OF ABSTRACT	20. LIMITATION OF ABSTRACT
UNCLASSIFIED	UNCLASSIFIED	UNCLASSIFIED	

NSN 7540-01-280-5500

DTIC QUALITY INSPECTED 1

Standard Form 298 (Rev. 2-89)
Prescribed by ANSI Std. Z39-18
298-102

DISCLAIMER NOTICE

THIS DOCUMENT IS BEST QUALITY AVAILABLE. THE COPY FURNISHED TO DTIC CONTAINED A SIGNIFICANT NUMBER OF PAGES WHICH DO NOT REPRODUCE LEGIBLY.

December 1995

University of Virginia

STRUCTURE AND DYNAMICS OF EXCITED ATOMS

Final
~~Annual~~ Report
Grant No. F49620-95-0034

15 November 1994 - 14 November 1995

by

T.F. Gallagher

Prepared for:

AIR FORCE OFFICE OF SCIENTIFIC RESEARCH
Building 410
Bolling Air Force Base
Washington, DC 20332

Attn: Dr. Ralph Kelley
General Physics Division
Directorate of Physics

Thomas F. Gallagher
Principal Investigator

Table of Contents

Appendices

I. Introduction

Our efforts under AFOSR grant F49620-95-1-0034 have been focused on two topics, resonant collisional energy transfer between cold Rydberg atoms and microwave multiphoton processes in Rydberg atoms. In both of these lines of research we are taking advantage of the exaggerated properties of Rydberg atoms to explore physical regimes which would be hard to study quantitatively in other systems. For example in the collision experiments with cold Rydberg atoms we hope to see the evolution from two body collisions to many body interactions as we increase the strength of the interaction between atoms.

II. Resonant Collisional Energy Transfer

During this grant period we have made significant progress toward our goal of studying cold, dense samples of Rydberg atoms. We trapped Rb atoms in a magneto optical trap using an inexpensive glass cell and diode lasers.[1] In the course of making the trap work we developed a sophisticated master-slave laser arrangement[2] in which only one laser, the master, is frequency locked to a saturated absorption line, and the others, the slave lasers, are injection locked to that laser, allowing essentially 100% optical efficiency of the slave lasers. Once the glass trap worked, and we were confident that we understood its parameters, we built a stainless steel vacuum system for the trap. It has now been working since June, 1995, and we have developed an imaging system which allows us to measure the size of the trapped atom cloud, and the number of trapped atoms. The cloud is 1 mm in diameter, and we estimate the atomic density to be 10^{10} cm^{-3}. Using the trap we have been able to observe good resonant collision signals for the process

$$\text{Rb nd} + \text{Rb nd} \rightarrow \text{Rb}(n+3)p + \text{Rb}(n-1)k, \tag{1}$$
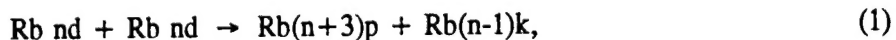
In Eq. (1) the (n-1)k state is a Stark state of principal quantum number n-1. The typical n values we have used are in the range $30 < n < 40$. We have observed the collisional resonances using electric field tuning, and at the moment the field inhomogeneties, which are $\sim$ 3 parts in 1000 are the major source

1

of the breadth of the collisional resonances. In spite of this broadening we are still able to see resonances as narrow as 30 MHz, far narrower than observed for the process of Eq. (1) in our beam apparatus. We are presently trying to see if we can observe collisions assisted by an rf field so we can dispense with the field tuning. In the long run we shall have to redesign the electrodes in the trap, but we would like to observe the intrinsic width of a collisional resonance without that effort first.

In this period we have finished the analysis of resonant collision lineshapes for different distributions of the velocities of the colliding atoms. We have found that whenever the velocity distribution is as wide as the average velocity the resulting lineshape is cusp shaped. Thus the velocity distributions for thermal atoms in a cell or an atomic beam give cusp shaped lines, as does a velocity distribution consisting of a single velocity group. In contrast, collisions between atoms in two distinct velocity groups lead to Lorentzian lineshapes. A report of this work is in preparation, and the abstract is included as Appendix A.

III. Microwave multiphoton processes

In the past year we have worked on several aspects of microwave multiphoton processes. Two of these projects were focused on the evolution of atomic states in changing microwave fields. In the first project we exposed Rydberg K atoms to microwave pulses which power shifted the atoms into or through multiphoton resonances.[3,4] By turning the microwaves on and off with different rise and fall times we verified that the atomic response could be described in terms of the atomic levels dressed by the microwave field. A report of this work has been published in Physical Review A and is included as Appendix B.

In many ways the most classical Rydberg atoms are those in the circular states, the states for which $\pm m = \ell = n-1$. They are difficult to prepare,[5,6] and we have in the past year reported a demonstration of a new, efficient way of producing circular states, the states for which $\pm m = \ell = n-1$.

Our method, which we have demonstrated with Na, is to excite the Rydberg atoms in a circularly polarized microwave field to the (n+1)s state for n ≃ 20. Although there are many other states within 1 cm^{-1} their optical excitation strength from the 3p state is negligible, and they are not excited. As the microwave fields is turned off the atoms initially in the (n+1)s state adiabatically traverse an avoided crossing with the adiabatic extension of the circular state of principal quantum number n, and are left in this state when the field reaches zero. Positive or negative m is selected by the choice of polarization of the microwave field. The method works very well, and a report has been published in Physical Review Letters and is included as Appendix C.

A subject of great theoretical interest is ionization by circularly polarized fields,[7,8] but there is only one experimental paper.[9] In the past year we have finally completed reports of the ionization of both Na and Li by 8 and 18 GHz circularly polarized fields. In the former experiments we have demonstrated that even at a frequency of 18 GHz the ionization field is well described by

$$E = 1/16n^4 \qquad (2)$$

is marked contrast to a theoretical estimate of the lower bound,[7] which is far lower. We have measured the sensitivity to ellipticity of the polarization and developed a simple, quantitative model to account for the observations. Finally, we have shown that small static fields in the plane of the rotating microwave field produce striking enhancements in the ionization. For both elliptical polarization and an applied static field the enhancement originates from resonant transitions between the rotating frame eigen states driven by the static field or the counter rotating component (for elliptical polarization). A report of this work has been submitted for publication and is included as Appendix D.

In the Li experiment we had hoped to see a striking difference between the $\ell + m$ even and $\ell + m$ odd states, because the latter are much more hydrogen like. Ionization of Na m=2 states by linearly polarized fields is very different from that of the m=0 and 1 states for this reason.[10] However the ionization of both sets of states occurs at essentially the same field, a somewhat disappointing, but none

the less enlightening result. An initially surprising result of the experiment was our ability to see clear structure in the excitation spectra of the $\ell+m$ odd states, excited via the np m=0 levels, but none in the $\ell+m$ even states excited via the np m=±1 levels. The difference is due to the energy shift of $+m\omega$ in transforming between the laboratory and rotating frames.[11] For m=0 there is no shift, but the m=±1 states, which are degenerate in the laboratory frame, are split by 2ω in the rotating frame of the field, doubling the number of observed lines and blurring the resulting spectrum. A report of this work has been submitted for publication, and the abstract is included as Appendix E.

For two years we have worked on making short rf and microwave pulses. We have made rf pulses at frequencies of 200-600 MHz specified numbers of cycles from one to fifty cycles. Using these rf pulses we have examined how a two level system, of K Rydberg states responds as the rf pulse is changed from one to many cycles. The objective is to connect recent half cycle pulse results[12] to conventional descriptions of resonance phenomena.[13] With one cycle we observe a fairly structureless response. With two cycles what was formerly unstructured exhibits interference fringes much like a Young's two slit interference pattern. With progressively more cycles the constructive interference maxima develop into sharp resonances, with many similarities to a diffraction pattern. What may be surprising is that the highly structured response to many cycles is implicit in the response to one cycle. We are now writing a report of this work.

We have also managed to make very short 8 GHz microwave pulses, only 0.5 ns long. These pulses contain only 4 field cycles, and present many novel opportunities. We have used them for microwave ionization of Na. With a 500 ns long pulse Na Rydberg states can be ionized by a field[10]

$$E = 1/3n^5, \tag{3}$$

which is the field at which the Stark manifolds of principal quantum number n and n+1 cross. As the pulse is shortened the ionization no longer exhibits a sharp onset at $E = 1/3n^5$ but exhibits a gradual rise. Finally, with a 0.5 ns pulse ionization does not occur until

4

$$E = 1/9n^4 \qquad (4)$$

as is true for H or high m H-like states. Even though the microwave field is strong enough to drive the Δn transitions required for ionization at the field $E=1/3n^5$, there are simply not enough field cycles to ionize the atoms. However, Δn transitions do occur, and with the shortest microwave pulses we find most of the population transferred to other states.

IV. Stark Avoided Crossings

We have started to use Rb for the trap experiments, and as a consequence, we need to be sure that we understand the spectroscopy in E fields and field ionization in Rb. For both of these reasons we have measured the avoided level crossings of the Rb (n+3)s states with lowest levels of the adjacent n Stark manifolds. We have found that the measured values agree with those computed by our matrix diagonalization program,[14] showing that it is indeed quite reliable. The measurements also prodded us to develop an analytical form for the magnitudes of avoided crossings between s states and the Stark states in the heavier alkali atoms K, Rb, and Cs. We were able to develop a perturbation theory expression showing the dependence on the quantum defects of the s states as well as well the n dependence. A report of this work has been submitted for publication, and the abstract is included as Appendix F.

V. Conclusion

In the past year we have started experiments in two areas; cold trapped Rydberg atoms, and short microwave pulses, which offer the promise of many new insights. We expect to realize these over the next few years.

References

1. C.H. Monroe, W. Swann, R. Robinson, and C.E. Wieman, Phys. Rev. Lett. 65, 1571 (1990).

2. J. Yu, M.-C. Gagne, C. Valenin, R.-L. Yuan, and P. Pillet, J. Phys. France III 2, 1615 (1992).

3. M. Baruch and T.F. Gallagher, Phys. Rev. Lett. 68, 3515 (1992).

4. S. Yoakum, L. Sirko, and P.M. Koch, Phys. Rev. Lett. 69, 1919 (1992).

5. R.G. Hulet and D. Kleppner, Phys. Rev. Lett. 51, 1430 (1983).

6. J. Hare, M. Gross, and P. Guy, Phys. Rev. Lett. 61, 1938 (1988).

7. M. Nauenberg, Phys. Rev. Lett. 64, 2731 (1990).

8. J.A. Griffiths and D. Farrelly, Phys. Rev. A45, R2678 (1992).

9. P. Fu, T.J. Scholz, J.M. Hettema, and T.F. Gallagher, Phys. Rev. Lett. 64, 511 (1990).

10. P. Pillet, H.B. van Linden van den Heuvell, W.W. Smith, R. Kachru, N.H. Tran, and T.F. Gallagher, Phys. Rev. A30, 280 (1984).

11. H. Salwen, Phys. Rev. 99, 1274 (1955).

12. R.R. Jones, D. You, and P.H. Bucksbaum, Phys. Rev. Lett. 70 1236 (1993).

13. J.H. Shirley, Phys. Rev. 138, B979 (1965).

14. M.L. Zimmerman, M.G. Littman, M.M. Koch, and D. Kleppner, Phys. Rev. A20, 2251 (1979).

Appendix A

Lineshape Analysis of Resonant

Energy Transfer Collisions

J. Veale, W. Anderson, M. Gatzke, M. Renn, and T.F. Gallagher

Department of Physics,

University of Virginia,

Charlottesville, Virginia 22901

(December 30, 1995)

Abstract

We have investigated the resonant collision process $26s+24d\rightarrow26p+25p$ in K, which occurs when the 26s and 24d states are tuned by a static electric field so that the intervals 26s-26p and 24d-25p are equal. Resonant collision lineshapes are observed and analyzed for three collision velocity distributions: a thermal beam, a small band of velocities in a laser cooled beam, and two well separated velocity groups in a laser cooled beam. Collisions between atoms with a broad distribution of relative velocities produce cusp lineshapes. In contrast, collisions occurring between atoms in two well defined velocity groups produce approximately Lorentzian lineshapes.

Quantum interference in microwave multiphoton transitions

M. Gatzke, R.B. Watkins, and T.F. Gallagher

Department of Physics, University of Virginia, Charlottesville, Virginia 22901

(Received 25 July 1994)

We observe interference in the resonant microwave multiphoton transition probability between the 21s state and the 19,3 Stark state of K in a static field as a function of the duration and intensity of a microwave pulse at 9 GHz. The 19,3 state adiabatically connects to the 19f state in zero field. The ac Stark effect shifts the 21s state through a multiphoton resonance with the 19,3 Stark state during both the rising and falling edges of the microwave pulse. The transitions that occur during each traversal of the resonance lead to an interference in the net transition probability as a function of the relative phase accumulated by each state during the pulse. We measure both the frequency of the interference oscillations for different detunings from resonance and the amplitude of the fringes for different degrees of pulse asymmetry. The latter results are in complete agreement with the predictions of a Landau-Zener model for the resonance transitions.

PACS number(s): 42.50.Hz, 32.80.−t

I. INTRODUCTION

Coherence has become an important aspect of many forms of laser manipulation of atoms and molecules. It plays an important role in both adiabatic cooling and compression [1,2], it is crucial to adiabatic population transfer in multilevel systems [3,4], and it has recently been shown to be important in multiphoton excitation and ionization using short pulses of both optical and microwave radiation [5–8].

The role of coherence in multiphoton excitation by a pulse of radiation is easily illustrated using a two-level example. Consider the model system with two levels (1 and 2) depicted in Fig. 1. Level 1 has an ac Stark shift so that the system is brought into a multiphoton resonance on the rising and falling edges of a radiation pulse. Suppose that initially only state 1 is populated. As the two levels pass through resonance on the rising edge of the pulse, a transition is made, creating a coherent superposition of states 1 and 2. This superposition evolves coherently in time until the resonance is traversed again during the falling edge of the pulse, where a second transition is made. When the pulse turns off the superposition state is projected onto the original states 1 and 2 with different amplitudes, depending on the relative phase accumulated by the states in the time between the two transitions. As indicated in Fig. 1, the net transition probability from state 1 to state 2 contains a contribution from evolution along two distinct paths resulting in interference. Consequently, varying the relative phase produces an interference pattern in the 1 to 2 transition probability. In this experiment the relative phase may be varied by changing either the width or the intensity of the radiation pulse. While such interference is difficult to observe with a pulsed laser due to the spatial variation of the beam intensity, it has recently been observed in several pulsed microwave experiments [7,8].

In this report we present an expanded study of interference from microwave multiphoton transitions between

the 21s state and the 19,3 Stark state of K in static electric fields. The 19,3 state is the one which adiabatically connects to the 19f state in zero field. We shall only be concerned with states which have orbital magnetic quan-
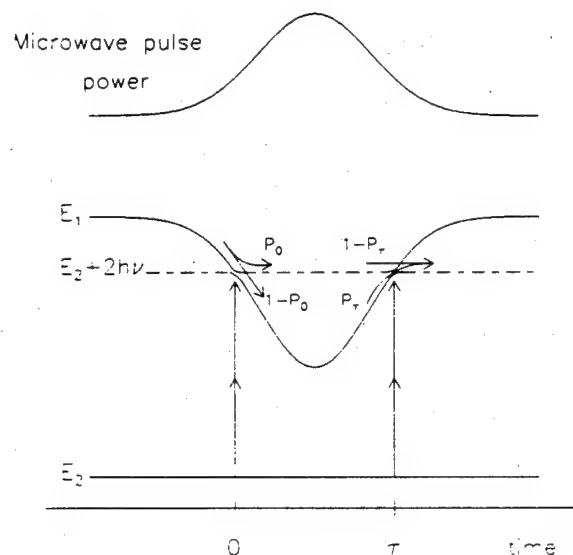

FIG. 1. Illustration of resonance transitions using a dressed-state picture. As the power in the microwave pulse rises and falls the ac Stark effect shifts state 1 into a two-photon resonance with state 2 twice at times $t = 0$ and $t = \tau$. The resonance is depicted as an avoided crossing of state 1 with a state which is obtained by *dressing* state 2 with two microwave photons. These two states have quasienergies $\epsilon_1 = \varepsilon_1$ and $\epsilon_2 = \varepsilon_2 + 2h\nu$, respectively, where ν is the frequency of the radiation and ε_1 and ε_2 are the real binding energies of the states 1 and 2. At the avoided crossings transitions take place between the states with the probabilities P_0 and P_τ as indicated. The width of the avoided crossing is the two-photon Rabi frequency. The relative dynamical phase Φ acquired by the states is the area bounded by the dressed states between the two avoided crossings.
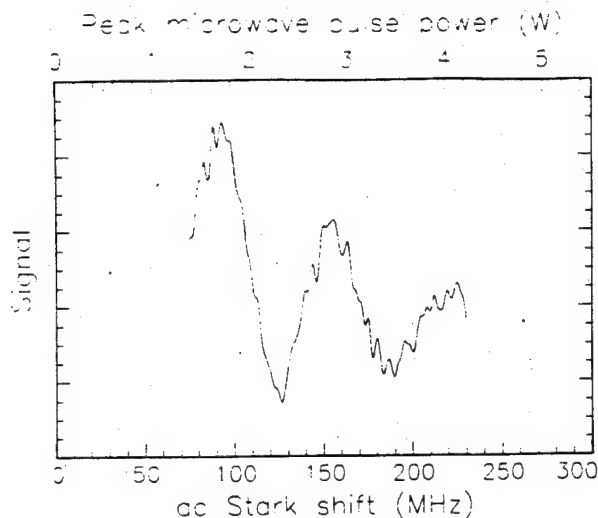
FIG. 2. The 19.3 Stark state field ionization signal plotted versus the ac Stark shift induced in the 21s state by the microwave field. Oscillations in the signal indicate interference in the resonant four-photon $21s \rightarrow 19.3$ transition probability.

tum number $m = 0$. In a microwave field, the 21s state has a small ac Stark shift due primarily to off-resonant interaction with the neighboring 20p and 21p states. In Fig. 1 it is represented by state 1. In our previous work we demonstrated interference in the 21s to 19.3 transition probability as a function of *detuning* from the four-photon 9 GHz microwave resonance [7]. In the experiments presented here we observe the interference as a function of the duration and intensity of the microwave pulse. Shown in Figs. 2 and 3 are scans of the 19.3
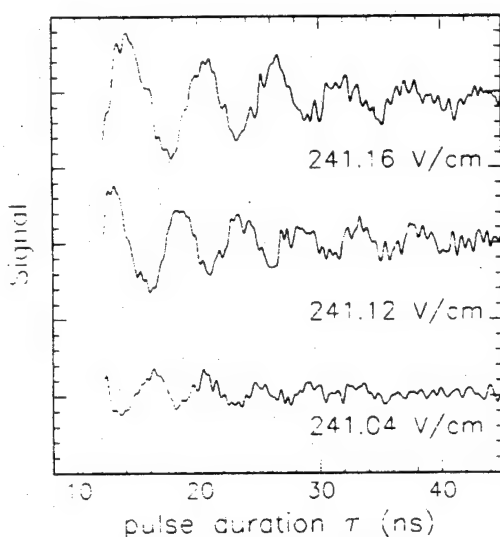

FIG. 3. The 19.3 Stark state field ionization signal plotted versus the duration [approximately the full width at half maximum (FWHM)] of the resonant microwave pulse for three different values of static field. The frequency of the interference oscillations is proportional to minus the detuning from the four-photon resonance with the 21s state at 239.5 V/cm, as explained in the text.

state population after laser excitation of the 21s state, obtained by selectively field ionizing the 19.3 state [9,10], as a function of the peak power (in Fig. 2) and the duration (in Fig. 3) of the microwave pulse. Oscillations in the signal reflect interference in the net transition amplitude. From interference patterns such as those of Fig. 3 we measure both the dependence of the interference oscillation frequency on the detuning from resonance, and the effect of an asymmetry between the rising and falling edges of the pulse on the amplitude of the interference fringes. The latter measurements are in agreement with the results predicted by a Landau-Zener model applied to Floquet or dressed states for the microwave multiphoton resonance transitions.

In the following sections we present a summary of the theory for two-state quantum interference, our experimental observations, and our conclusions.

II. THEORY OF TWO-STATE QUANTUM INTERFERENCE

As outlined in Sec. I, the observation of quantum interference between two atomic states requires that transitions between the states occur at two instances which are separated in time resulting in two distinct paths to each final state. In addition, the evolution of the states in the meantime must be coherent, preserving the relative phase between the states. One final requirement for observing interference is some method of selective state preparation and detection. In this section we derive a general expression describing the interference pattern produced by the arrangement depicted in Fig. 1, which is independent of the details of a particular experiment.

To produce the interference phenomenon discussed here, transitions between the states take place during the rising and falling edges of a microwave pulse with an electric field large enough to produce substantial ac Stark shifts of the atomic levels. Transitions occur whenever the levels are shifted back and forth through a multiphoton resonance as the intensity rises and falls during the pulse. It has been demonstrated both theoretically [12] and experimentally [10,7,8] that the evolution of atomic states in an intense resonant radiation field can be described by semiclassical Floquet theory as the evolution of atomic Floquet modes, or dressed atomic levels. In this model the multiphoton resonance is manifested as an avoided level crossing of the atoms' dressed states, as illustrated in Fig. 1, and the traversal of the avoided crossing results in a transition between the states. The parameter characterizing the coupling strength for the transition is the multiphoton Rabi frequency, which is simply the size of the dressed-state avoided crossing.

This situation is completely analogous to the case of slow inelastic atomic collisions in which avoided crossings of the molecular levels are traversed as the internuclear distance changes during the collision. This problem was treated by Landau, Zener, and Stückelberg [13], and the theory of transitions during avoided level crossings is referred to as Landau-Zener theory. Oscillations in the inelastic molecular cross sections, which appear as a re-

sult of interference between the level crossings traversed during the incoming and outgoing phases of the collision, are referred to as Stückelberg oscillations.

In Landau-Zener theory, the evolution of the states during the traversal of an avoided crossing can be expressed in terms of a unitary evolution operator

$$T = \begin{pmatrix} \sqrt{1-P} & \sqrt{P}e^{-i\phi} \\ -\sqrt{P}e^{i\phi} & \sqrt{1-P} \end{pmatrix}, \qquad (1)$$

where P is the (adiabatic) transition probability and ϕ is a phase shift. Under certain conditions P and ϕ exhibit a simple dependence on the multiphoton Rabi frequency ν_n and the rate of traversal of the dressed level avoided crossing,

$$\dot{\nu} = \frac{1}{h}\frac{d}{dt}[\epsilon_2(t) - \epsilon_1(t)]. \qquad (2)$$

Here, $\epsilon_1(t)$ and $\epsilon_2(t)$ are the dressed-state quasienergies of the two states, which are time dependent during the

avoided crossing traversal. In Landau-Zener theory, the traversal is assumed to begin at infinite detuning and end at infinite detuning on the other side of resonance and is assumed to occur at a constant rate $\dot{\nu}$. In this case, P and ϕ can both be expressed in terms of a single parameter γ_n, defined as

$$\gamma_n \equiv \frac{\nu_n^2}{4\dot{\nu}}. \qquad (3)$$

The resulting expression for P is [13]

$$P = 1 - e^{-2\pi\gamma_n}. \qquad (4)$$

The unitary transition matrix $\mathcal{T}$ which describes the net transition probability resulting from the situation depicted in Fig. 1 is the product of a Landau-Zener transition matrix T_0, for the rising edge of the pulse at time $t = 0$, a free evolution propagator U from $t = 0$ to $t = \tau$, and finally another Landau-Zener matrix T_τ^{-1} for the transitions during the falling edge at $t = \tau$,

$$\mathcal{T} = T_\tau^{-1} U T_0$$
$$= \begin{pmatrix} \sqrt{1-P_\tau} & \sqrt{P_\tau}e^{-i\phi_\tau} \\ -\sqrt{P_\tau}e^{i\phi_\tau} & \sqrt{1-P_\tau} \end{pmatrix}^{-1} \begin{pmatrix} e^{-i\int_0^\tau \frac{\epsilon_1(t)}{\hbar}dt} & 0 \\ 0 & e^{-i\int_0^\tau \frac{\epsilon_2(t)}{\hbar}dt} \end{pmatrix} \begin{pmatrix} \sqrt{1-P_0} & \sqrt{P_0}e^{-i\phi_0} \\ -\sqrt{P_0}e^{i\phi_0} & \sqrt{1-P_0} \end{pmatrix}. \qquad (5)$$

The net $1 \to 2$ transition probability P_{12} is then simply $|\mathcal{T}_{12}|^2 = |\mathcal{T}_{21}|^2$. From Eq. (5) above, the result for P_{12} is the sum of two terms, one representing the incoherent sum of the net transition probabilities via the two distinct paths connecting the initial and final states illustrated in Fig. 1, and a corresponding interference term,

$$P_{12} = [P_0(1 - P_\tau) + P_\tau(1 - P_0)]$$
$$-2\sqrt{P_0(1 - P_\tau)P_\tau(1 - P_0)}$$
$$\times \cos[\Phi + (\phi_0 - \phi_\tau)]. \qquad (6)$$

The interference term oscillates as a function of the relative dynamical phase acquired during the time between the transitions at the rising and falling edges of the pulse. In Floquet theory dynamical phase reflects the quasienergy difference of the dressed states,

$$\Phi(\tau) = \frac{1}{\hbar}\int_0^\tau dt[\epsilon_1(t) - \epsilon_2(t)]. \qquad (7)$$

We have considered so far the general case where there are separate transition probabilities P_0 and P_τ, as well as different phase shifts ϕ_0 and ϕ_τ, during the rising and falling edges of the pulse. If the pulse is temporally symmetric, then $P_0 = P_\tau = P$, $\phi_0 = \phi_\tau$, and

$$P_{12} = 4P(1 - P)\sin^2\left(\frac{\Phi}{2}\right). \qquad (8)$$

It should be noted that an essential requirement for a Floquet description of pulsed experiments is that the

modulation of the radiation during the pulse be slow compared to the frequency of the radiation. This is called the adiabatic approximation, and it is assumed to be valid for the experiments discussed here. Otherwise, Floquet theory must be modified to account for nonadiabatic transitions induced by the rapid modulation of the radiation [12].

In our presentation of the theory for quantum interference an artificial distinction has been made between the resonant transition events and free evolution. This was required in order to describe the net transition probability in such a simple fashion. In effect, we have treated the transitions as if they occur essentially instantaneously (and discontinuously) compared to the time between the transitions. While this is a good approximation of the situation for the experiments discussed in this work, it is possible to generate quantum interference even when it is not. In such cases the dynamical phase ϕ acquired during the transitions cannot be distinguished from the freely evolving phase and the transition matrix $\mathcal{T}$ cannot be conveniently separated as it is in Eq. (5). In fact, interference may still be observed even in cases where the states are never completely uncoupled, and the coherent superposition is never evolving *freely*, although there may not be a simple analytic expression describing the interference pattern generated.

III. EXPERIMENTAL APPROACH

We observe quantum interference between two atomic Rydberg states of K which are coupled by a microwave

radiation field. In this experiment, which is an exact analogy of the ideal pulsed laser experiment, a microwave resonance is driven between two states of the atom during the rising and falling edges of a microwave pulse. We rely on the ac Stark shift to tune the 21s state in and out of a four-microwave-photon resonance with an $n = 19$ Stark state during the radiation pulse [10]. The interference patterns published in our initial study were generated in this way [7].

For this experiment we required microwave pulses with well defined and controlled temporal profiles. Using a double balanced mixer (Watkins Johnson M14A) whose intermediate frequency port was driven by a computer controlled HP 8112A pulse generator with a variable rise time, we could amplitude modulate the microwave signal from a sweep oscillator with a pulse shape determined largely by the trapezoidal wave form from the pulse generator. These pulses, which were only slightly distorted from a trapezoidal shape due to the limited frequency response of our mixers, were then amplified by a broad band traveling wave tube amplifier. The 0.7 mW of broad band (8–12 GHz) noise power generated by the amplifier resulted in a maximum microwave signal to noise ratio of 38 dB [11]. In our original version of the experiment a high Q resonant cavity was used [7]. However, the microwave pulse's temporal wave form inside a cavity is determined by the exponential filling or damping time of the radiation in the cavity. In order to preserve the shape of the applied wave form, in the present experiment we used a section of ordinary rectangular waveguide (WR 137) operated in the TE_{10} mode near 9 GHz. By measuring the field inside the waveguide section of the microwave line using a probe we find a voltage standing wave ratio (VSWR) of 2.0 ± 0.1 at an operating frequency of 8.8 GHz. In addition, we simultaneously measured the power transmitted through the line in order to calibrate the microwave field inside the waveguide. The uncertainties associated with these measurements result in an estimated uncertainty of $\pm 20\%$ for the microwave field used in our experiments. The waveguide was terminated, after about 30 dB attenuation, at a waveguide-mounted mixer/detector (HP 11521A), where the wave form was analyzed. Despite the relatively large VSWR we observed approximately trapezoidal pulses as short as 8 ns full width at half maximum (FWHM) intensity with a minimum rise time (10–90 % of peak intensity) of 5 ns. However, for very short pulses of duration approaching the round trip time in the waveguide (about 1 ns), the effects of poor coupling should significantly alter the pulse wave form.

Except for the microwave transmission scheme, the general experimental setup is identical to that of the previously published work [7] so only a sketch is presented here. Inside an evacuated chamber K atoms from an atomic beam entered the waveguide from a small hole in one of the side walls, and two laser beams tuned to the 4s-4p and 4p-21s transitions entered from an identical hole on the other side. These holes in the waveguide (including another at the top) have diameters of less than 1/30 of the microwave wavelength and were observed to have no effect on the microwave transmission properties of the

system. In addition, numerical estimates of the field distortions produced by the hole in the top of the waveguide are less than 1% over the interaction region near the center of the waveguide. The lasers excited the atoms inside the waveguide in the presence of a static electric field produced by applying voltage to a copper plate or septum fitted into the waveguide perpendicular to the microwave electric field. At specific values of the static field, the 21s state and members of the $n = 19, l \geq 3$ manifold of Stark states are resonantly coupled by the microwave field [10]. A sketch of the Stark effect for these two atomic levels is shown in Fig. 4. This experiment focuses on the four-photon resonance between the 21s state and the lowest energy (19,3) Stark state which occurs in a field of about 240 V/cm. Resonant transitions are detected by selectively field ionizing the Rydberg atoms [9]. The atoms are ionized by appling a high voltage pulse to the septum inside the waveguide. It is possible to distinguish between the ionization signals produced by either the 21s state or the 19,3 Stark state by selecting the peak field of this ionization pulse so that only the Stark state atoms, which have a lower field ionization threshold, are ionized. The
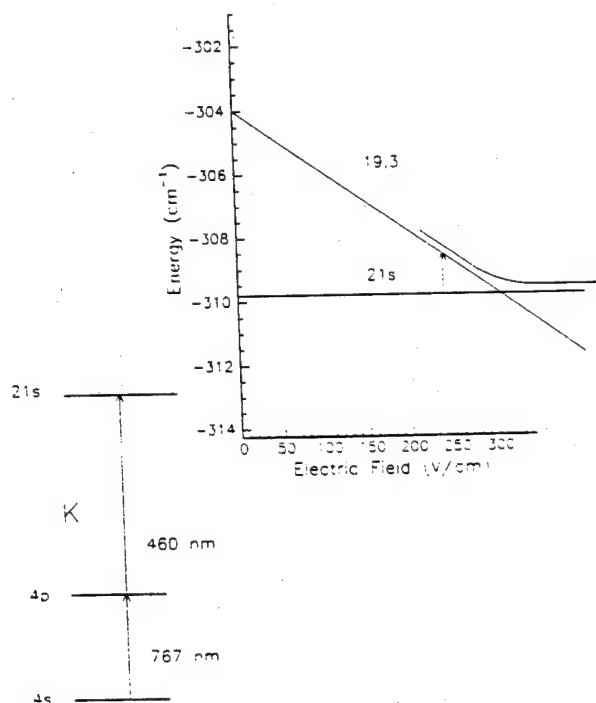

FIG. 4. A sketch of the atomic levels in K which are relevant for this experiment. Two-step laser excitation through the 4p state from the 4s ground state is used to selectively populate the 21s state in a static electric field near a value where it is resonant with the higher-lying 19,3 Stark state in a 9 GHz microwave field. Transitions are detected by selectively ionizing the 21s and 19,3 states with an electric field pulse. This pulse rises slowly enough to allow adiabatic traversal of the avoided crossing at 304 V/cm so that the Stark state remains less bound and therefore easier to ionize than the 21s state.

ions then exit the waveguide through a hole in the top and are detected using microchannel plates. The signal detected in the interference patterns shown in Figs. 2, 3, and 5 is the 19.3 Stark state ionization signal, which is proportional to the $21s \to 19,3$ transition probability.

IV. RESULTS AND DISCUSSION

In our previous studies of interference in microwave multiphoton transitions between K Rydberg states, the results were compared to numerical calculations of the transition probability [7]. The reason for this was the fact that the time dependence of the microwave pulse was not simple, making an analytic expression for the net transition probability difficult to obtain. In the related experiment performed using He Rydberg atoms, the interference was observed as a function of quasienergy difference during the pulse by varying the pulse intensity [8]. Even though the pulse shape was well known, analytic expressions for the transition probability are complicated, and only numerical results were used for comparison with the data. We have subsequently reproduced interference by this same method for multiphoton resonances in K using our trapezoidal pulses, as shown in Fig. 2. In this case, the analytic expression for the net transition probability given in Eq. (6) is valid. However, it is complicated because the dynamical phase Φ of Eq. (7) depends not only on the quasienergies but also on the time τ between the traversals of resonance, both of which change with the changing pulse intensity. In addition, not only is Φ a complicated function of pulse intensity, but the individual transition probabilities P_0 and P_τ of Eq. (4) are also functions of the pulse intensity through the changing pulse rise and fall times. The end result is an analytical expression for the transition probability P_{12} as a function of pulse intensity which is so complicated that results from numerical integration of the two-state Schrödinger equation are no less useful as a theoretical comparison.

In contrast, the interference pattern shown in Fig. 3 is far simpler to interpret. In this case interference is generated simply by varying the duration of the microwave pulse τ, which we define here as the time between traversals of the dressed-state avoided crossings during the rising and falling edges of the pulse, as indicated in Fig. 1. In this scenario the rise and fall times of the pulse and therefore the transition probabilities P_0 and P_τ are unchanged. Hence, the only dependence of P_{12} on pulse duration is through the dynamical phase, and that dependence is linear, $\Phi(\tau) = \Delta\tau - \Phi_0$, where Δ is the quasienergy difference at the peak of the microwave pulse, and $-\Phi_0$ accounts for the small constant dynamical phase which is not accumulated during the rising and falling edges of the pulse because the temporal wave form of the pulse is trapezoidal and not square. Therefore, with our well controlled microwave pulses it is possible to generate interference patterns which are easily interpreted using our model described in Sec. II. In this section we present interference patterns along with measurements of both the oscillation frequency as a function

of detuning and the oscillation amplitude as a function of pulse transition time, and we compare these results with the predictions of our model according to Eqs. (4)–(7).

Shown in Fig. 3 are interference patterns generated by changing the pulse duration for three different detunings from resonance, i.e., static fields. The frequency of the oscillations $d\Phi/d\tau = \Delta$ is the difference between the $21s$ state and Stark state quasienergies at the peak of the pulse,

$$\Delta = \frac{1}{\hbar}(\delta\epsilon_{21s} - \epsilon_{19}) = \frac{\delta\epsilon_{21s}}{\hbar} - 2\pi k(E - E_0). \qquad (9)$$

Here $\delta\epsilon_{21s}$ is the ac Stark shift of the $21s$ state during the peak of the microwave pulse, $E - E_0$ is the detuning from the four-photon resonance in the limit of no ac Stark shift at $E_0 = 239.5$ V/cm, and k is the difference between the static dipole moment of the Stark state and that of the $21s$ state induced by the static field E_0. As evident in Fig. 3, the oscillation frequency decreases with increasing field E in agreement with the prediction of Eq. (9). Fitting the oscillation frequency to the static field, we arrive at a best fit of $k = 552$ MHz/(V/cm), in good agreement with a theoretical prediction, 558 MHz/(V/cm), calculated by a direct diagonalization of the Rydberg atom Hamiltonian in an electric field [10]. The result for the other fitted parameter $\delta\epsilon_{21s}/\hbar + 2\pi k E_0$ is also in agreement with our measurements, although the uncertainty in determining the peak ac Stark shift is more than 10%.

Before proceeding to our measurements of the amplitude of the interference fringes, we note that damping is clearly present in the interference patterns of Fig. 3. The theory presented in Sec. II does not take into account the effect of experimental inhomogeneities which produce damping. Because of inhomogeneity in the applied static field E, different atoms within the sample have different quasienergy differences, and hence different dynamical phases and different interference oscillation frequencies according to Eq. (9). The total signal from all atoms is therefore a sum over interference patterns with slightly different oscillation frequencies, resulting in the damping evident in Fig. 3. The measured damping time of these interference patterns, denoted T_2^* in accordance with magnetic resonance terminology, is approximately 30 ns. Although the exact inhomogeneous distribution of electric fields experienced by our sample of atoms is unknown, T_2^* can be used to define an approximate inhomogeneous width in electric field,

$$\delta E \simeq \frac{1}{4kT_2^*} \simeq 16\,\text{mV/cm}, \qquad (10)$$

which agrees very well with the measured width of our narrowest microwave resonances.

Finally, we investigated the effect of asymmetry on the interference pattern. Shown in Fig. 5 are the results for three pulses with the same 6 ns fall time but different rise times: 15 ns, 30 ns, and 40 ns. In the first signal trace the interference oscillations are initially almost as large as the average transition probability (the contrast of the fringes is high) while in the signal traces for the more asymmetric pulses the oscillations are reduced relative

to the average signal level. Figure 6 is a plot of the amplitudes of the oscillations for the interference patterns of Fig. 5, as a function of the pulse rise time, normalized by the incoherent (time average) transition probability which we obtained by averaging out the oscillations. In all three traces shown in Fig. 5 we have renormalized the signal to make this average transition probability equal to 1/2. The oscillations are fit including a damping factor, and the fit values for the initial undamped amplitudes are used for the plot in Fig. 6. The curve through the data in Fig. 6 is the prediction of Eq. (6) for the ratio

(interference oscillation amplitude)
‾‾‾‾‾‾‾‾‾‾‾‾‾‾‾‾‾‾‾‾‾‾‾‾‾‾‾
(average transition probability)

$$= \frac{2\sqrt{P_0(1-P_\tau)P_\tau(1-P_0)}}{P_0(1-P_\tau) + P_\tau(1-P_0)}, \quad (11)$$

FIG. 6. Our measurements and a theoretical prediction for the ratio of the amplitude of the interference oscillations to the time average transition probability for signals similar to those shown in Fig. 5 as a function of the microwave pulse rise time. In all cases the pulse fall time was 6 ns.
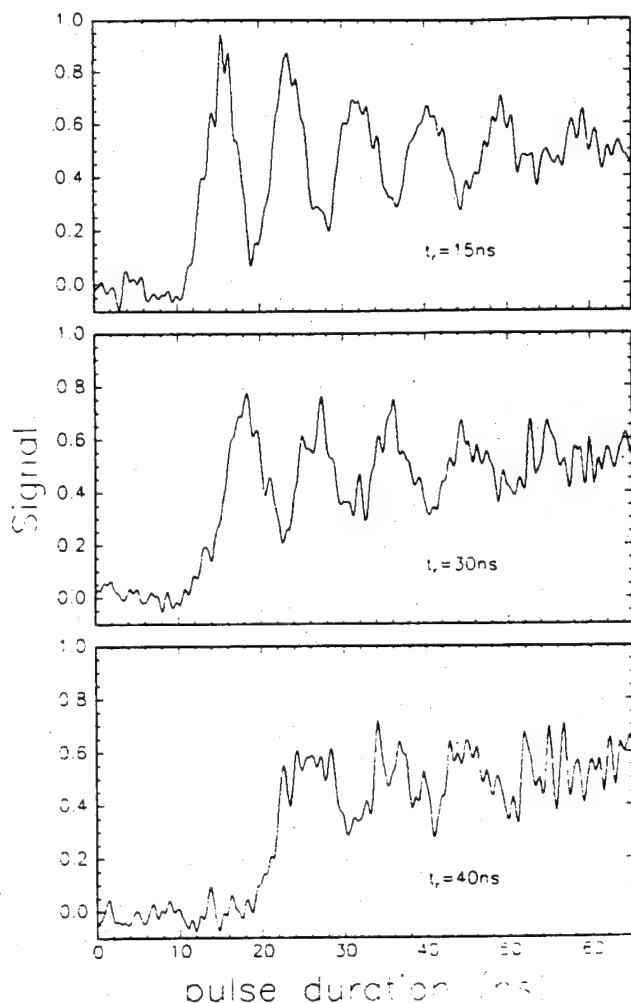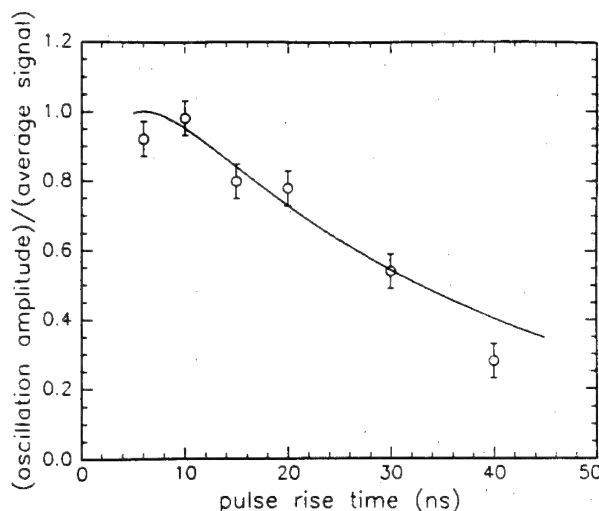

FIG. 5. The 19,3 Stark state field ionization signal plotted versus the microwave pulse duration (FWHM) for three different resonant microwave pulses, all having a 6 ns fall time and rise times of 15 ns, 30 ns, and 40 ns. Clearly, the more asymmetric the pulse, the less contrast there is in the interference fringes, in accordance with Eq. (11).

where P_0 and P_τ according to Landau-Zener theory are given by Eq. (4). As is true of quantum interference in general, the incoherent transition probability is simply the algebraic sum of the transition probabilities for each of the two paths connecting the initial and final states, while the amplitude of the interference oscillations is twice the geometric mean of the transition probabilities for the two paths.

A single parameter is required to produce the theoretical curve in Fig. 6, a scaling factor relating the pulse rise time t_r to the Landau-Zener parameter,

$$\gamma_4 = \left(\frac{h\nu_4^2}{\delta\epsilon_{21s}}\right) t_r, \quad (12)$$

where ν_4 is the four-photon Rabi frequency (the size of the dressed-state avoided crossing) and $\delta\epsilon_{21s}$ is the ac Stark shift of the 21s state at the peak of the pulse. The value of the scale parameter for these interference patterns, $h\nu_4^2/\delta\epsilon_{21s} = 12$ MHz, is determined by two independent measurements: the detuning from the resonance field E_0 and either the peak power of the microwave pulse, or the peak ac Stark shift of the 21s state, which are related by

$$\frac{\epsilon_{21s}}{h} = \frac{\alpha E_{rf}^2}{4}. \quad (13)$$

Here $\alpha = 0.195$ MHz/(V/cm)^2 is the polarizability of the 21s state. We are able to determine the ac Stark shift of the 21s state by simply observing the shift of the resonance using a method which is described in our earlier work [10]. The result is $\epsilon_{21s}/h \simeq 250$ MHz. This is in excellent agreement with our measured value of the

maximum microwave field. $E_{rf} = 70$ V/cm, which implies $\epsilon_{21s}/h \simeq 240$ MHz. The detuning from resonance is determined most accurately by combining Eq. (9) with our measured ac Stark shift and measuring the frequency of the interference oscillations. For the trapezoidal pulses employed in this experiment, the oscillation frequency Δ from Eq. (9) is the ac Stark shift from the point in the pulse where the avoided crossing is traversed to the peak of the pulse. The measured value $\Delta = 115$ MHz can then be used to determine the microwave field at the point in the pulse where the avoided crossing occurred. about 53 V/cm. Finally, from previous measurements of the multiphoton Rabi frequency of this transition as a function of microwave field [10], we can predict the avoided crossing to be $\nu_4 = 55$ MHz, and therefore arrive at the prediction for the scaling parameter $h\nu_4^2/\delta\epsilon_{21s} = 12$ MHz. The agreement of this prediction with our measurements shown in Fig. 6 is clearly within our experimental uncertainty. We therefore conclude that the validity of our model is demonstrated by the interference patterns observed in these experiments.

evolution of two ordinary atomic levels. Specifically, we have shown that when the ac Stark shift produced by a radiation pulse shifts two levels into a multiphoton resonance on both the rising and falling edges of the pulse. interference is clearly observable in the transition probability due to the coherence of the evolution during the pulse. We have shown that the interference pattern depends on the duration, intensity, and temporal symmetry of the pulse in a predictable way. Interference in the transition probability can only be observed if the coherence of the superposition state formed after the resonance is traversed on the rising edge of the pulse is preserved until the resonance traversal on the falling edge. As the pulse is lengthened, inhomogeneities in the static field begin to destroy the coherence and damp the interference fringes.

Although we have performed these experiments with well controlled microwave pulses. the evolution in a laser pulse is essentially the same as long as the adiabatic condition is met. Consequently, the Floquet approach described here is widely applicable to the analysis of multiphoton processes driven by pulsed lasers.

V. CONCLUSIONS

This work demonstrates that, when the adiabatic condition is met, the coherent evolution of two Floquet levels in response to a changing ac Stark shift is identical to the

ACKNOWLEDGMENT

[1] P. Pillet. C. Valentin, R.-L. Yuan. and J. Yu, Phys. Rev. A 48. 845 (1993).
[2] P. Marte, P. Zoller, and J.L. Hall, Phys. Rev. A 44, 4118 (1991).
[3] B. Broers, H.B. van Linden van den Heuvell. and L.D. Noordam. Phys. Rev. Lett. 69, 2062 (1993).
[4] U. Gaubatz, P. Rudecki, S. Schiemann, and K. Bergmann, J. Chem. Phys. 92, 5363 (1990).
[5] R.B. Vrijen. J.H. Hoogenraad, H.G. Muller, and L.D. Noordam, Phys. Rev. Lett. 70. 3016 (1993).
[6] J.G. Story, D.I. Duncan, and T.F. Gallagher. Phys. Rev. Lett. 70, 3012 (1993).
[7] M.C. Baruch and T.F. Gallagher. Phys. Rev. Lett. 68, 3515 (1992).
[8] S. Yoakum. L. Sirko, and P.M. Koch. Phys. Rev. Lett. 69 1919 (1992); L. Sirko, S. Yoakum, A. Haffmans, and P.M. Koch. Phys. Rev. A 47, R782 (1993).
[9] T.F. Gallagher, L.M. Humphrey, W.E. Cooke. R.M. Hill, and S.A. Edelstein, Phys. Rev. A 16, 1098 (1977).
[10] M. Gatzke, M. Baruch, R.B. Watkins, and T.F. Gallagher, Phys. Rev. A 48, 4742 (1993).
[11] Based on the work described in [8], we do not expect any distortion of the interference oscillations as a result of this level of broad band amplifier noise. There the authors report no observable effects for a microwave signal to noise ratio of greater than 30 dB from noise in a 13.5 GHz band.
[12] H.P. Breuer, K. Dietz, and M. Holthaus. Z. Phys. 8, 349 (1988); 10, 13 (1988); H.P. Breuer and M. Holthaus, Phys. Lett. A 140, 507 (1989).
[13] L. Landau, Phys. Z. Sowjetunion 1, 46 (1932); C. Zener, Proc. R. Soc. London Ser. A 137, 696 (1932); E.C.G. Stückelberg, Helv. Phys. Acta 5, 369 (1932).

Production of Circular Rydberg States with Circularly Polarized Microwave Fields

C. H. Cheng, C. Y. Lee, and T. F. Gallagher

Department of Physics, University of Virginia, Charlottesville, Virginia 22901
(Received 18 July 1994)

We describe an experimental method of producing circular Rydberg states using a circularly polarized microwave field. A Na s state is excited in the circularly polarized microwave field, and as the field is turned off, it makes an adiabatic rapid passage through a multiphoton resonance and evolves adiabatically into the circular state. Minimal optical selectivity is required and the field can be turned off quickly.

Circular Rydberg atoms, those with $|m| = l = n - 1$, are required for a diverse set of experiments focused on the Rydberg constant [1], collision cross sections [2], cavity quantum electrodynamics [3,4], and stabilization against ionization by strong electromagnetic fields [5]. Here n, l, and m are the principal, angular momentum, and azimuthal orbital angular momentum quantum numbers. Circular states are not optically accessible from low lying atomic states, and, to date, two methods have been used to prepare them. The first is the adiabatic rapid passage method of Hulet and Kleppner [6]. They ramped a static field in the presence of a perpendicular oscillating field to convert an optically accessible Rydberg state of Li to the $n = 19$ circular state by a sequence of adiabatic rapid passages through single photon resonances. Nussenzvieg *et al.* have recently shown how this technique may be extended to $n = 50$ states by adding a small magnetic field [7]. The second approach is the crossed field approach suggested by Delande and Gay [8] and first realized by Hare *et al.* [9]. Atoms are excited to the highest energy Stark state in a strong electric field and pass adiabatically into a region of weak electric field and a perpendicular strong magnetic field. The atoms remain in the highest energy state, which is the circular state in the magnetic field.

Here we report the use of a new method to produce spatially oriented circular states of Na. A Na s state is excited in a circularly polarized microwave field, and as the field is turned off, it makes an adiabatic rapid passage through a single multiphoton resonance and evolves into the circular state. This method differs from the method of Hulet and Kleppner [6] in having a single adiabatic rapid passage rather than a sequence of them, and it is a variant of a proposal to use the circularly polarized fields by Molander *et al.* [10]. The principle of the method is easily understood if we transform the problem to a frame rotating with the microwave field so that the field is static and does not drive transitions. Consider a field which has amplitude E, lies in the horizontal x-y plane, and rotates about the z axis at angular frequency ω in the laboratory frame. The phase of the field is chosen so that it lies along the $+x$ axis in the rotating

frame. To find the eigenenergies and states in the rotating frame, we first transform the zero field Na eigenstates to the rotating frame. A zero field Na nlm state with energy W has a laboratory frame wave function given in atomic units by $\Psi_{nlm}(\bar{r}, t) = R(r)\Theta(\theta)e^{im\phi}e^{-iWt}$, where r, θ, and ϕ are the Rydberg electron's polar coordinates relative to the Na$^-$. Explicitly, r is the distance, θ is the polar angle relative to the z direction, and ϕ is the azimuthal angle. Using the rotating frame coordinates r_R, θ_R, and ϕ_R, where $r = r_R$, $\theta = \theta_R$, and $\phi = \phi_R + \omega t$, we can rewrite the wave function as $\psi_{nlm}(\bar{r}, t) = R(r_R)\Theta(\theta_R)e^{im\phi_R}e^{-i(W-m\omega)t}$. The spatial wave function is unchanged, but there is an energy shift of $-m\omega$ [11,12]. Using these wave functions, we can diagonalize the Hamiltonian matrix in the rotating frame with an added field term, using the same procedures used for static fields [13]. Unlike a static field, m is not conserved, but $l + m$ is either even or odd.

In Fig. 1 we show the energy levels of the $l + m$ even Na states near $n = 21$ as a function of the amplitude of a field rotating at a frequency of $\omega/2\pi = 8.026$ GHz. As shown by Fig. 1, the zero field levels are displaced by $-m\omega$, so the transformation to the rotating frame has the same effect as adding a B field of ω/μ_0, where μ_0 is the Bohr magneton. As the field is increased from zero, the Stark effect splits the levels emanating from the high l $n = 21$ states, and the lowest energy Stark state, which is the adiabatic continuation of the circular $m = l = 20$ state, apparently crosses the $22s$ state at $E = 252$ V/cm. In fact, there is an avoided crossing, and the separation of the levels is computed to be 210 MHz, as shown by the inset of Fig. 1.

The basic notion of the experiment is to excite the Na atoms with a pulsed dye laser from the $3p$ state to the $22s$ state at a field between the first two avoided crossings, at 252 and 277 V/cm. The field is then reduced slowly to a field below the first avoided crossing, traversing the avoided crossing in a time long compared to $1/210$ MHz, to ensure an adiabatic rapid passage from the $22s$ state to the lowest energy Stark state. Finally, the field is reduced more rapidly to zero, and the Stark state evolves adiabatically into the circular state. The last step can be
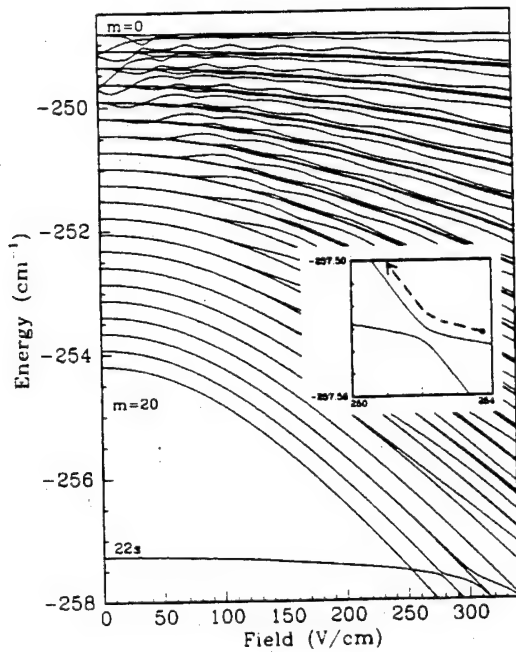
FIG. 1. The Na $22s$ and $n = 21$ $m \geq 0$ energy levels in a frame rotating at 8.026 GHz as a function of the rotating 8.026 GHz field amplitude. The displacement of the levels by $-m\omega$ is quite evident. The lowest Stark state, which is the adiabatic continuation of the zero field circular $n = 21, l = m = 20$ state apparently crosses the $22s$ state at 252 V/cm. As shown in the inset, there is an avoided crossing. To produce the $n = 21$, circular state atoms are excited to the $22s$ state at a field of 255 V/cm; then the field is slowly reduced through the avoided crossing to produce an adiabatic passage to the lowest Stark state; then as the field is more rapidly reduced to zero and the Stark state evolves into the circular state.

done rather quickly since the zero field states are 8 GHz apart. The last step of this method is essentially the proposal of Molander et al. [10], and the mathematical similarity of their method to the crossed field method has been pointed out by Chen et al. [14]. The major attractions of our method are twofold. First, the laser bandwidth and power requirements are minimal. Only the $22s$ state absorbs the laser light, so even though our laser bandwidth of 0.9 cm^{-1} overlaps several Stark states, it does not matter since they do not absorb the light. Also, very nearly the full $3p$-$22s$ oscillator strength is available. Second, the process can be quick, because of the 8 GHz level separation in the rotating frame. As a result, the atoms do not move far, and very little redistribution due to blackbody radiation occurs, even at room temperature [15]. If the sense of field rotation is reversed, the $m = -l$ circular state is populated instead of the $m = +l$ state.

To produce a circular state and verify its identity requires that we be able to produce and turn off a circularly polarized field in the x-y plane and then apply a pulsed ionizing field in the z direction. While an open Fabry-Pérot cavity should meet the microwave requirements [12], it is awkward for field ionization, and

we have used a cylindrical cavity instead. It is constructed of two identical brass halves with the cavity symmetry axis vertical, in the z direction, as shown in Fig. 2. The inside length and diameter of the cavity are 1.98 and 6.40 cm, and the separation between the two halves is 0.51 cm. We operate the cavity on two degenerate TE$_{111}$ modes at a frequency of 8.026 GHz. On the axis of the cavity one has its E field in the x direction and the other in the y direction. By driving the x and y polarized modes to produce fields with the same amplitude and a 90° relative phase shift we produce a circularly polarized field in the x-y plane. The orthogonally polarized fields are coupled into the cavity through 6.68 mm diameter irises in the top and bottom of the cavity from orthogonally polarized waveguides. Each waveguide is cut off to the other polarization, minimizing the coupling between the cavity modes. When the cavity is aligned there is a 0.3 MHz difference in the center frequencies of the modes, and their Q's are 3519 and 3535. The Q's must be very nearly the same, or the field in the cavity rapidly becomes elliptically polarized as the modes decay.

To allow the application of an ionizing field in the z direction we insulate the feed waveguide from the bottom half of the cavity with a 0.5 mm thick teflon sheet. It allows us to put up to 11 kV on the lower half of the cavity leading to ionizing fields as high as 5.5 kV/cm, enough to ionize circular states of $n \geq 20$. Electrons ejected from atoms at the center of the cavity pass through the iris in the upper cavity half and through a 2 mm diameter hole in the upper feed waveguide, as shown in Fig. 2.

The microwave power originates in a Hewlett-Packard (HP) 83620A synthesized sweep oscillator which is kept at 8.026 GHz. The power level is controlled externally. The output of the oscillator is amplified in a Litton 624 gated traveling wave tube amplifier which can produce up to 100 W. The output of the amplifier is split into two
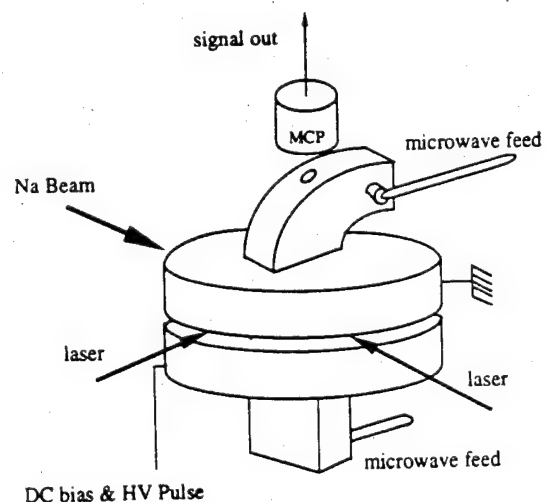

FIG. 2. Schematic diagram of the apparatus.

arms to feed the x and y polarized cavity modes. One arm contains an HP X885A phase shifter, an HP 8495 0–70 dB step attenuator, and a 20 dB directional coupler with an HP 432A power meter. The second arm contains a Waveline 622 precision rotary vane attenuator. There is a circulator in each arm just before it enters the vacuum chamber. With this arrangement we are able to produce circularly polarized fields in the cavity with an amplitude of 1100 V/cm and measure them with an accuracy of 7.3%.

In the experiment a Na beam passes between the two halves of the cavity, as shown by Fig. 2. The atoms are excited by two pulsed dye laser beams, which also pass between the two halves of the cavity. One beam, tuned to the 3s-3p transition at 589 nm, crosses the Na beam at a right angle 1.6 mm upstream from the center of the cavity. The second beam, tuned to the 3p-22s transition at 414 nm, is perpendicular to the first and counterpropagating to the atomic beam. The timing sequence of the experiment is as follows. The lasers fire at time $t = 0$ μs. The oscillator is turned on at $t = -8$ μs, and the amplifier is gated on for 4.6 μs starting at $t = -4$ μs, so the field in the cavity is at a steady state value of 255 V/cm when the lasers fire. The power of the oscillator is reduced linearly between $t = 10$ ns and $t = 600$ ns, and the field in the cavity drops from 255 to 173 V/cm during this time. This time is long enough that more than 98% of the atoms should pass adiabatically from the 22s state to the lowest Stark state. At $t = 600$ ns the oscillator is turned off, and the field in the cavity decays with the cavity time constant of 70 ns. The field ionization pulse begins at $t = 1.6$ μs and has a 700 ns rise time. We detect electrons from atoms ionized by the field pulse with the microchannel plate detector shown in Fig. 2. The arrival time of the electrons implies the ionizing field, and the calibration is checked using the known ionization fields of the Na ns states. The signal from the microchannel plates goes to a digital oscilloscope and a gated integrator. The whole procedure is repeated at the 10 Hz repetition rate of the laser. Typically, a small static field of 2.5 V/cm in the z direction is present, and the magnetic field is less than 10 mG.

Using the timing sequence outlined above, we have excited the Na 22s state at three different peak microwave fields, below, at, and above the avoided crossing with the lowest $n = 21$ Stark state. Experimentally, we find the avoided crossing at 247 V/cm, not at 252 V/cm as shown in Fig. 1, but well within the uncertainty of the field measurement. To minimize confusion in comparisons to Fig. 1 we give all experimental microwave fields after multiplying them by 252/247. In Fig. 3 we show the resulting field ionization signals. With $E = 249$ V/cm, below the avoided crossing, the field ionization signal, shown in Fig. 3(a), is identical to that of the 22s state in zero field. At $E = 252$ V/cm, the field of the avoided crossing, we excite both states with the laser and there are
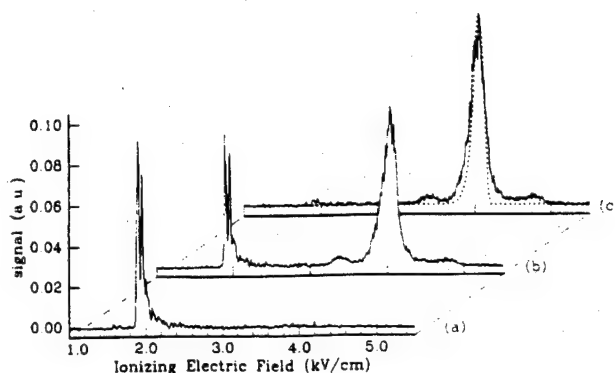

FIG. 3. The field ionization signals when the 22s state is excited in three different circularly polarized microwave field amplitudes. (a) For $E = 249$ V/cm, below the avoided crossing, only the 22s field ionization signal at $E_I = 1.92$ kV/cm is visible. (b) For $E = 252$ V/cm, at the avoided crossing: half the signal is in the 22s state and half is in the $n = 21$ circular state, at $E_I = 4.06$ kV/cm. (c) $E = 255$ V/cm, above the avoided crossing, nearly all the signal matches the calculated ionization signal for the $n = 21$ circular state shown by the dotted line. The small peaks at $E_I = 3.4$ and 4.8 kV/cm are attributed to the $n = 20$ and 22 circular states. The signals of (b) and (c) are multiplied by three relative to the signal in (a): the number of atoms detected is the same in all three cases.

two features in the field ionization signal, one due to the 22s state and one due to the $n = 21$ circular state. Finally, at $E = 255$ V/cm, a field above the avoided crossing with the lowest Stark state but below the next one, is, by far, the largest feature visible in the $n = 21$ circular state, as shown in Fig. 3(c). It is in excellent agreement with the signal calculated using the hydrogenic ionization rates of Damburg and Kolosov [16] and the 8×10^9 V/cm s slew rate of our ionizing pulse. In Fig. 3(c), the 22s signal has almost vanished, but there are small signals peaked at 3.4 and 4.8 kV/cm, the ionization fields of the $n = 20$ and 22 circular states, which are populated from the $n = 21$ circular state by blackbody radiation [15]. When the field is raised beyond $E = 273$ V/cm, transfer to lower l and m states of $n = 21$ begins to occur. Comparing the areas under the signals of Fig. 3(c) we find that 1% of the atoms remain in the 22s state and 90% are left in the $n = 21$ circular state. Of the remaining 9%, 4% and 5% are transferred to the $n = 20$ and 22 circular states, respectively, by blackbody radiation [15]. If the apparatus were cooled, 99% of the atoms would presumably be left in the $n = 21$ circular state.

The tolerances of the method constitute an important factor in determining its usefulness. From the level diagram of Fig. 1 it is apparent that the field amplitude must be between the first and second anticrossings. The microwave field must be controlled to $\pm 9\%$ and the power to $\pm 18\%$ (0.7 dB), not a terribly stringent requirement. On the other hand, ellipticity in the polarization due to imperfect phase and amplitude adjustments can be a problem. Ellipticity adds a field oscillating at 2ω in the

rotating frame. and this field can drive resonant transitions between the states of Fig. 1. In Fig. 4 we show the field ionization signals with the correct amplitudes of both modes. $E = 260$ V/cm. but with phase errors of $\Phi = 3°$. $5.5°$. and $7.5°$ from circular polarization. A phase error of $-\Phi$ leads to the same field ionization signal as $+\Phi$. The circular state signal is unchanged with a $\pm 3°$ phase error and is reduced by half with $\pm 5.5°$ of phase error. which corresponds to an oscillating field with 5% of the amplitude of the rotating field. With a phase error of $\pm 7.5°$, the fraction of atoms left in the circular state is markedly diminished. Keeping the phase error to $\pm 3\%$ is not particularly difficult. Ellipticity caused by amplitude error has comparable effects. When the power into one of the arms is changed by ± 0.5 dB from circular polarization. the signal from the circular state is diminished by half. A 0.5 dB error corresponds to an oscillating field amplitude which is 6% of the rotating field amplitude. We attribute the deleterious effects of ellipticity to processes occurring at high fields near the avoided crossings. While we have little direct experimental evidence. we presume that when the Stark shifts are less than the frequency. ellipticity is not a severe problem. This notion is supported by the calculations of Molander et al. [10]. which indicate that ellipticity is tolerable in the regime well below the avoided crossing with the s state. A static field of ± 2.5 V/cm in the z direction is always adequate to overcome stray fields. With field it is not necessary to cancel the Earth's magnetic field.

With an operating frequency of 8.026 GHz and rotating fields of 255 and 366 V/cm we have observed the production of $n = 21$ and $n = 20$ circular states. We cannot produce $n \geq 22$ circular states since their avoided crossings with the $(n + 1)s$ states occur at such low fields that they are too small to be usable. A lower frequency would alleviate this problem. We have observed the complete depopulation of the $18s-21s$ states at fields within 3% of the calculated fields of their a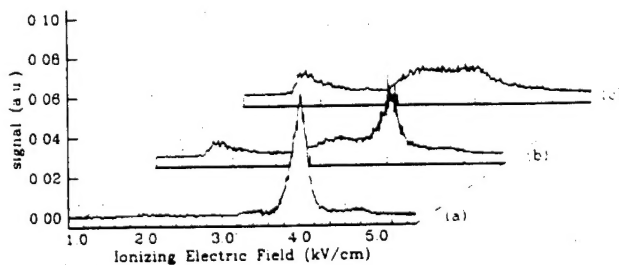voided crossings with the lowest Stark states which are the adiabatic continuations of the $n = 17-20$ circular states. We think we are producing these circular states. but we cannot explicitly observe them because we cannot field ionize them. With our maximum microwave field of 1100 V/cm at 8.026 GHz we cannot depopulate the $17s$ state. However. the same field at 9.4 GHz would be adequate to depopulate it.

In conclusion. the technique described here is an efficient and rapid way of producing circular states. It is quite general and can be optimized for a range of n by the choice of microwave frequency. With minor modifications it should also be possible to produce elliptic states using this approach. although it is less natural than using the crossed field method [17].

FIG. 4. Field ionization signals with a field amplitude of 255 V/cm and three phase detunings Φ from circular polarization (a) $\Phi = 3°$: the circular state production is unchanged from Fig. 3(c). (b) $\Phi = 5.5°$: the circular state production is reduced by half. (c) $\Phi = 7.5°$: most atoms are left in states other than the circular state.

[1] S. Paine, P. Chang, R. Lutwak, J. Holley, and D. Kleppner. Bull Am. Phys. Soc. **37**. 1117 (1992).

[2] S. B. Hansen, T. Ehrenreich, E. Horsdal-Pedersen, K. B. MacAdam, and L. J. Dube, Phys. Rev. Lett. **71**, 1522 (1993).

[3] M. Brune, P. Nussenzveig, F. Schmid-Kaler, F. Bernadot, A. Maali, J. M. Raimond, and S. Haroche, Phys. Rev. Lett. **72**, 3339 (1994).

[4] R. G. Hulet, E. S. Hilfer, and D. Kleppner. Phys. Rev. Lett. **55**, 2137 (1985).

[5] M. P. deBoer, J. H. Hoogenraad, R. B. Vrijen, L. D. Noordam, and H. G. Muller, Phys. Rev. Lett. **71**, 3263 (1993).

[6] R. G. Hulet and D. Kleppner, Phys. Rev. Lett. **51**, 1430 (1983).

[7] P. Nussenzveig, F. Bernadot, M. Brune, J. Hare, J. M. Raimond, S. Haroche, and W. Gawlik, Phys. Rev. A **48**, 3991 (1993).

[8] D. Delande and J. C. Gay, Europhys. Lett. **5**, 303 (1988).

[9] J. Hare, M. Gross, and P. Goy, Phys. Rev. Lett. **61**, 1938 (1988).

[10] W. A. Molander, C. R. Stroud, Jr., and J. A. Yeazell. J. Phys. B **19**, L461 (1986).

[11] H. Salwen, Phys. Rev. **99**, 1274 (1955).

[12] P. Fu, T. J. Scholz, J. M. Hettema, and T. F. Gallagher, Phys. Rev. Lett. **64**, 511 (1990).

[13] M. L. Zimmerman, M. G. Littman, M. M. Kash, and D. Kleppner, Phys. Rev. A **20**, 2251 (1979).

[14] L. Chen, M. Cheret, F. Roussel, and G. Spiess, J. Phys. B **26**, L437 (1993).

[15] T. F. Gallagher, in *Rydberg States of Atoms and Molecules*, edited by F. B. Dunning and R. F. Stebbings (Cambridge University Press, Cambridge, 1983).

[16] R. J. Damburg and V. V. Kolosov, in *Rydberg States of Atoms and Molecules*, edited by R. F. Stebbings and F. B. Dunning (Cambridge University Press, Cambridge, 1983).

[17] J. C. Day, T. Ehrenreich, S. B. Hansen, E. Horsdal-Pedersen, K. S. Mogesen, and K. Taulbjerg, Phys. Rev. Lett. **72**, 1612 (1994).

Circularly and Elliptically Polarized Microwave Ionization of Na Rydberg Atoms

C. Y. Lee, J. M. Hettema, C. H. Cheng, C. W. S. Conover,*

and T. F. Gallagher

Department of Physics

University of Virginia

Charlottesville, VA 22901

Abstract

The 17.3 GHz circularly polarized microwave ionization (CPMI) threshold fields for Na Rydberg atoms are measured and compared to the previous 8.5 GHz measurements. The experimental approach to producing the circularly polarized microwave field is to use a Fabry-Perot cavity. An angular momentum barrier model is proposed to describe the threshold field measurements of CPMI, and the maximum amount of angular momentum which can be transferred in a circularly polarized microwave field is deduced from the experimental data. Elliptically polarized microwave ionization (EPMI) of Rydberg atoms and CPMI in the presence of a small static field are studied with microwave frequencies of approximately 8 Ghz and 17 GHz. Unexpected resonant peaks at microwave fields below the CPMI threshold fields are observed in both cases at 8, but not at 17, GHz. A sequence of resonant microwave transitions is proposed to explain these resonant structures in EPMI and CPMI in the presence of a small static field.

Appendix E

Ionization of Li Rydberg Atoms by 8.5 and 18 GHz Circularly Polarized Microwave Fields

C.H. Cheng, C.Y. Lee, and T.F. Gallagher
Department of Physics
University of Virginia
Charlottesville, VA 22901

Abstract

We have measured separately the ionization threshold fields of the sets of Li states composed of $\ell + m$ even and $\ell + m$ odd zero field states. In spite of the fact that the states composed of $\ell + m$ even states are, by one measure, more non hydrogenic than those composed of the $\ell + m$ odd states, we observe that both sets of states ionize in a microwave field $E \approx 1/16n^4$, as do Na atoms. This field is well below the hydrogenic ionization field. The ionization of the states composed of $\ell + m$ odd states shows that small departures from hydrogen lead to completely non hydrogenic ionization, as in a static field. In contrast, in a linearly polarized microwave field small departures from hydrogen do not lead to non hydrogenic ionization. The excitation spectrum of the states composed of $\ell + m$ odd states exhibits regular structure, while that of the states composed of $\ell + m$ even states does not, a difference due to the differing energy shifts accompanying transformations between the laboratory and rotating frames.

Avoided level crossings between s states and Stark states in Rydberg Rb atoms

M. Gatzke, J.R. Veale, W.R. Swindell, and T.F. Gallagher

Department of Physics, University of Virginia, Charlottesville, Virginia 22901

(August 16, 1995)

Abstract

We have measured the locations and widths of the avoided level crossings between $(n+3)$s states and nk Stark states in Rydberg Rb atoms with principal quantum numbers n between 16 and 25. We used two-step laser excitation to excite $(n+3)$s states in the presence of an electric field, and we observed a change in the rate of blackbody-radiation-driven transitions to higher lying states as the electric field is tuned through the avoided level crossings. Final state analysis is performed using pulsed field ionization. By recording the field ionization signal as a function of electric field we have measured both the positions and widths of the avoided crossings. We show that the magnitudes of this type of avoided crossing, which occurs in K, Rb, Cs, can be calculated using a perturbation theory approach based on incomplete Stark manifolds. In addition to providing the magnitudes of the avoided crossings, this approach displays their dependence on principal quantum number and quantum defect.